RESEARCH PAPERS

Acta Cryst. (1998). B**54**, 197–203

Structural Analysis of Cs_2HgBr_4 in Normal, Incommensurate and Twinned Phases

CARLOS BASÍLIO PINHEIRO,* ADO JÓRIO, MARCOS ASSUNÇÃO PIMENTA AND NIVALDO LÚCIO SPEZIALI

Departamento de Física, ICEx-UFMG, Brazil. E-mail: basilio@fisica.ufmg.bn

(*Received 1 April 1997; accepted 11 September 1997*)

Abstract

X-ray diffraction and Raman spectroscopy experiments have been used to investigate different phases of Cs_2HgBr_4, dicesium mercury tetrabromide, from room temperature to 213 K. Structural analyses have shown that the crystal could be described, in the normal and in the incommensurate phases, both by ordered and disordered models, but the latter gave more consistent results. Raman results corroborate the descriptions based on X-ray analysis; the presence of an extra peak, which according to group theory should be forbidden in an ordered structure, indicates the lack of local symmetry and was associated with an orientational disorder of $[HgBr_4]^{2-}$ tetrahedra. In the transition from the incommensurate to the commensurate phase a multi-soliton behavior was observed. The Cs_2HgBr_4 crystal in the low-temperature commensurate phase is composed of two types of ordered pseudomerohedral twinned domains.

1. Introduction

The compounds classified in the well known A_2BX_4 family are generally considered as candidates to present modulated structures in their phase-transition sequence. Some α-K_2SO_4-related crystals have been shown to present disordered structures with the X atoms occupying two very close positions (Aleksandrov, 1993). Among those exhibiting modulated phases two compounds, Cs_2CdBr_4 and Cs_2HgBr_4, are special; their phase transition from the incommensurate to the commensurate phase occurs at $\mathbf{q} = 0$, *i.e.* without the appearance of a superstructure (Altermatt *et al.*, 1979)

Cs_2CdBr_4 crystals present four different phases on cooling from room temperature

Pnma		*Pnma*		$P2_1/n$		$P\bar{1}$
$Z = 4$		$Z = 4$		$Z = 4$		$Z = 4$
$\longrightarrow$	T_1	$\longleftrightarrow$	T_2	$\longleftrightarrow$	T_3	$\longleftarrow$
	(252 K)		(237 K)		(158 K)	
RT		INC		LT_1		LT_2
		$\mathbf{q} = 0.17\mathbf{a}^*$		Twinned		

The structural phase transformations were characterized by changes in the orientation of the $[CdBr_4]^{2-}$ tetrahedra. In general, no significant modifications in the internal structure of the tetrahedron could be noted in all phases. The Cs_2CdBr_4 room-temperature (RT) structure is isomorphous to β-K_2SO_4 (space group *Pnma*): Cd, both Cs and two Br atoms are in the *.m.* mirror plane and the other two Br atoms are related to one another by this symmetry element. A projection along the *a* axis makes evident a pseudohexagonal aspect of the structure. In the RT phase the existence of static disorder was excluded by the unique NQR signal (Altermatt *et al.*, 1984). Between 252 and 237 K weak satellite reflections were observed and this phase (INC) could be well described as incommensurate in the *Pnma*($\bar{1}ss$) space group (Speziali & Chapuis, 1989). The INC structure is described by a rotation wave of the $[CdBr_4]^{2-}$ tetrahedra around the **a** axis with an amplitude of almost 7°. After the INC $\rightarrow$ LT_1 phase transition the crystal structure is described in the $P2_1/n$ space group with two pseudomerohedral twinned domains. In each domain the $[CdBr_4]^{2-}$ tetrahedra are simultaneously rotated by ~7° around the **a** axis with a slight displacement in the **b** direction.

Phase transitions in Cs_2HgBr_4 were first observed by Semin *et al.* (1978), using NQR experiments.

According to Altermatt *et al.* (1984) Cs_2HgBr_4 presents a phase-transformation sequence similar to that presented by Cs_2CdBr_4 with an extra phase transition, leading to one more low-temperature phase (LT_3).

So far, no reference to structural disorder in Cs_2HgBr_4 and Cs_2CdBr_4 crystals have been made. Pakhomov *et al.* (1978) refined the RT phase of Cs_2HrBr_4 in the *Pnma* space group and found a large distortion in the $[HgBr_4]^{2-}$ ion.

© 1998 International Union of Crystallography
Printed in Great Britain – all rights reserved

Table 1. *Cs_2HgBr_4 crystal data and data collection parameters in the different phases studied*

Crystal data				
Chemical formula		Cs_2HgBr_4		
M_r		786.02		
	Phase I (RT)		Phase II (INC_{av})	Phase III (LT_1)
Cell setting	Orthorhombic	Orthorhombic	Orthorhombic	Monoclinic
Space group	$Pn2_1a$	$Pnma$	$Pnma$	$P2_1/n$
a (Å)	10.243 (2)	10.270 (2)	10.240 (1)	10.231 (1)
b (Å)	7.923 (1)	7.946 (1)	7.900 (1)	7.873 (1)
c (Å)	13.890 (2)	13.935 (2)	13.888 (1)	13.906 (1)
α (°)				90.000 (7)
V (Å^3)	1127.2 (3)	1137.1 (3)	1123.5 (3)	1120.1 (2)
Z	4	4	4	4
D_x (Mg m^{-3})	4.630	4.590	4.645	4.660
Radiation type	Mo $K\alpha$	Ag $K\alpha$	Ag $K\alpha$	Ag $K\alpha$
λ (Å)	0.7107	0.5608	0.5608	0.5608
No. of reflections for cell measurement	40	55	50	65
2θ range (°)	10–20	15–30	15–30	15–30
Crystal shape, color		Spherical, transparent		
Crystal size, radius (mm)	0.14 (1)	0.065 (5)	0.065 (5)	0.065 (5)
μ (mm^{-1})	34.12	18.22	19.07	18.50
Measurement temperature (K)	295	295	230	213
Data collection				
Diffractometer type		Siemens P4		
Data collection method		$\theta/2\theta$		
Absorption correction type		Spherical		
	Phase I (RT)		Phase II (INC_{av})	Phase III (LT_1)
T_{max}	0.024	0.184	0.180	0.180
T_{min}	0.0072	0.170	0.165	0.166
No. of reflections measured	1548	4053	849	1250
No. of independent reflections	1419	1604	775	1250
No. of observed reflections [$I > 3\sigma(I)$]	1320	768	726	1223
R_{int}	0.033	0.055	–	–
Maximum value of θ (°)	25	22.5	22.5	22.5
Range of h, k, l	$-12 \rightarrow h \rightarrow 13$	$-9 \rightarrow h \rightarrow 14$	$0 \rightarrow h \rightarrow 13$	$0 \rightarrow h \rightarrow 13$
	$-10 \rightarrow k \rightarrow 13$	$0 \rightarrow k \rightarrow 10$	$0 \rightarrow k \rightarrow 10$	$0 \rightarrow k \rightarrow 9$
	$-18 \rightarrow l \rightarrow 18$	$-18 \rightarrow l \rightarrow 18$	$0 \rightarrow l \rightarrow 18$	$-17 \rightarrow l \rightarrow 18$
No. of standard reflections	3	3	3	3

In the present work Cs_2HgBr_4 was systematically studied in three different phases using X-ray diffraction. A number of samples have been used in different data collections employing Ag $K\alpha$, Mo $K\alpha$ and Cu $K\alpha$ radiation. DSC (differential scanning calorimetry) measurements were used to identify the phase-transition temperatures. The RT phase was exhaustively investigated and structural descriptions based on ordered, disordered and anharmonic vibration models in $Pnma$ and $Pn2_1a$ have been tried. The average structure of the INC phase was investigated in a similar way to that used in the RT phase and the temperature dependence of the modulation vector could be observed.

2. Experimental

The first attempts to study the Cs_2HgBr_4 structures in different phases considered the total similarity between this compound and Cs_2CdBr_4, and the same crystallographic structures in the phase transformation were assumed for both. Single crystals of Cs_2HgBr_4 were grown from the melt using the Bridgman technique. The phase-transition temperatures were confirmed by DSC experiments using single crystals and powder samples; a small hysteresis was verified in T_2 [T_2 = 232.1 (2) K on cooling and T_2 = 234.4 (2) K on heating].

Different Cs_2HgBr_4 spherical samples with radii 0.065 (5) and 0.14 (1) mm were prepared for all the X-ray experiments. Diffraction measurements were performed on a four-circle diffractometer (Siemens P4) with graphite-monochromated radiation. Data collections were performed using *XSCANS* (Fait, 1991) software, employing intensity-dependent scan speeds in the θ–2θ scan mode. In order to investigate the crystal structure at different low temperatures, samples were cooled by a stream of nitrogen gas; the temperature stability was better than 0.5 K. In the RT phase data collection was performed at 295 (2) K, in the INC phase at 238.0 (5) K and in the LT_1 phase at 213.0 (5) K. The lattice parameters in all measurements were determined by a least-squares fit of 40 or more reflections (depending on the phase) in the range $0.233 \leq \sin\theta/\lambda \leq 0.462$.

Different X-ray radiation was used in the diffraction measurements. For structural studies of all the phases

Table 2. *Correlation diagram for the internal modes of Cs_2HgBr_4 in the RT phase*

Molecule point group (T_d43m)	Site group ($\sigma - m$)	Crystal point group ($D_{2h}mmm$)		
$A_1(\nu_1)$	A	A_{1g}	(x^2, y^2, z^2)	$\nu_1, 2\nu_3, \nu_2, 2\nu_4$
		B_{1g}	(xy)	ν_3, ν_2, ν_4
$E(\nu_2)$		B_{2g}	(xz)	$\nu_1, 2\nu_3, \nu_2, 2\nu_4$
		B_{3g}	(yz)	ν_3, ν_2, ν_4
T_1	B	A_{1u}		ν_3, ν_2, ν_4
		B_{1u}		$\nu_1, 2\nu_3, \nu_2, \nu_4$
$T_2(\nu_3, \nu_4)$		B_{2u}		ν_3, ν_2, ν_4
		B_{3u}		$\nu_1, 2\nu_3, \nu_2, 2\nu_4$

(RT, INC and LT_1) Ag $K\alpha$ radiation was employed in order to minimize the absorption effects ($\mu_{Ag\ K\alpha} \simeq 19\ mm^{-1}$). In order to analyze the anomalous scattering effect in the RT phase, and consequently the existence of a symmetry center in the structure, 774 Friedel pairs [$I \geq 3\sigma(I)$] were collected using Mo $K\alpha$ radiation ($\mu_{Mo\ K\alpha} \simeq 35\ mm^{-1}$). Owing to the small value of **q** (~0.17**a***) Cu $K\alpha$ radiation ($\mu_{Cu\ K\alpha} \simeq 93\ mm^{-1}$) was used in the study of the satellite reflection behavior between T_1 and T_2.

Data reduction was performed using *DATARED* and structure refinements were performed using *REFINE*, both programs from the *JANA*96 Crystallographic Computing System (Petricek & Dusek, 1996). A spherical absorption correction, according to the wavelength used in the different measurements, was applied to all the data. The functional wR† was refined in the full-matrix mode. Ordered and disordered models have been refined in all the phases. Harmonic and anharmonic atomic displacement refinements were also performed.

Table 1 shows a summary of crystal data and data collection parameters in RT, INC and LT_1 phases.

3. Results

3.1. *RT and INC_{av} structures*

Results found in the literature consider Cs_2HgBr_4 as isomorphous to Cs_2CdBr_4 with *Pnma* symmetry at room temperature. Group-theory analysis shows that these compounds present 81 optical modes in this phase, from which 60 are internal and 30 are active in Raman. Table 2 shows a diagram which correlates the $\bar{4}3m$ (T_d) point group of the free $[HgBr_4]^{2-}$ ion, the site group $m(C_s)$ and the factor group $mmm(D_{2h})$ of the crystal. The number and assignment of the internal modes associated with each irreducible representation of the $mmm(D_{2h})$ point group is given in the right-hand side of this table. In an ordered structure the ν_1 breathing mode of B_{1g} and B_{3g} representations would not be observed in a (xy) scattering geometry and only one stretching mode (ν_3) could be present, owing to the fact that the $[HgBr_4]^{2-}$ ion is placed in sites with *.m.* symmetry (Dmitriev *et al.*, 1989). In Cs_2HgBr_4 crystals the internal stretching mode should be observed in the 130–230 cm^{-1} interval. Nevertheless, Raman experiments have shown an unexpected result: two peaks with practically the same intensity are observed in this interval for B_{1g} and B_{3g} symmetries (Fig. 1). One of the peaks is associated with ν_3 (162 cm^{-1}) and the extra one is associated with the ν_1 mode (179 cm^{-1}). This result violates the previous group-theory analysis. It could be stated that there is a local symmetry break related to an orientational disorder of $[HgBr_4]^{2-}$ tetrahedra. The complete Raman analysis has been reported by Jório *et al.* (1998).

In order to decide which structure, in agreement with Raman results, better describes Cs_2HgBr_4 crystals, different models were considered in the X-ray measurements refinements: a disordered structure described in the space group *Pnma* ($Pnma_{des}$), an ordered structure described in the space group $Pn2_1a$ ($Pn2_1a_{ord}$) and a disordered structure described in space group $Pn2_1a$ ($Pn2_1a_{des}$). In the $Pnma_{des}$ model the two Br atoms, which in an ordered model should be placed on the *.m.* mirror plane, are assumed to be out of the plane; the other two Br atoms in the Br^4 tetrahedron

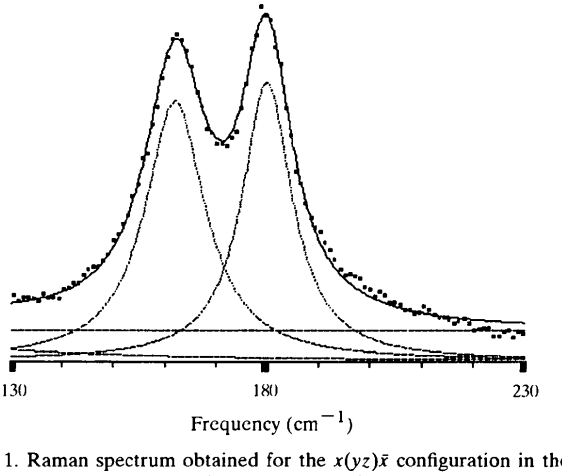

Fig. 1. Raman spectrum obtained for the $x(yz)\bar{x}$ configuration in the range of internal modes in the RT (290 K) phase: the presence of the peak at 179 cm^{-1}, ν_1 mode, violates the group-theory prediction.

† $wR = \sum w|F_o - F_c|^2 / \sum wF_o^2$.

Table 3. *Results obtained in Cs_2HgBr_4 structure refinements*

$Pn2_1a_{ord}$ and $Pnma_{ord}$ refinements in the RT phase are presented for the sake of comparison. All the refinements used data collected with Ag $K\alpha$ radiation.

Data collection	Phase I (RT, 295 K)			Phase II (INC_{av}, 235 K)	Phase III (LT, 213 K)
	$Pn2_1a_{ord}$	$Pnma_{ord}$	$Pnma_{des}$	$Pnma_{des}$	$P2_1/n_{ord}$
Use of	F	F	F	F	F
R	0.0414	0.0454	0.0410	0.0413	0.0363
wR	0.0347	0.0376	0.0333	0.0490	0.0411
S	1.14	1.31	1.13	1.60	1.42
Reflections used in refinement	1604	1604	1604	775	1223
No. of parameters refined	65	41	56	56	67
Weighting scheme	$1/\sigma(F)$	$1/\sigma(F)$	$1/\sigma(F)$	$1/\sigma(F)$	$1/\sigma(F)$
Maximum Δ/e.s.d.	0.0111	0.0005	0.0005	0.0001	0.0002
$\Delta\rho_{max}$	3.3	3.3	3.3	7.7	8.7
$\Delta\rho_{min}$	−4.7	−3.9	−3.9	−7.1	−8.2
Extinction correction type II	0.55 (5)	0.67 (5)	0.63 (5)	0.53 (5)	0.39 (6)
X parameter or twin volume ratio	0.5 (2)	–	–	–	0.41 (4)
Atomic scattering factors	*International Tables For Crystallography* (1992, Vol. C)				
Computer programs used	*JANA*96 (Petricek & Dusek, 1996)				

are no longer related by this symmetry element. As a consequence, a second tetrahedron is generated and the occupation parameter for these atoms had to be considered as $\frac{1}{2}$. In the $Pn2_1a_{des}$ model two Br tetrahedra were refined independently; refinement of occupation parameters for Br atoms converged to almost $\frac{1}{2}$. Attempts to split Cs and Hg positions did not converge and, for this reason, in all the disordered models these atoms were kept on the mirror plane.

The first structural studies were developed using large data sets collected with Ag $K\alpha$ radiation, containing few Friedel pairs. All the refinements considering the previously stated models clearly indicated that the crystal has a disordered structure in RT and INC phases. However, no relevant differences could be found between the results in noncentrosymmetric and centrosymmetric space groups, mainly if one considers that the increase in the number of refined parameters generally improves the agreement parameters.

Structure refinements of the $Pn2_1a_{ord}$ model using the set of Friedel pairs measured with Mo $K\alpha$, without averaging $I(\mathbf{h})$ and $I(\bar{\mathbf{h}})$, have shown that two sets of atomic positions related by *.m.* give the same results for the agreement parameters. The refinement of the Flack parameter (Flack, 1983) for the set of Friedel pairs, measured with Mo $K\alpha$, converged to $x = 0.46\,(4)$, indicating that in the noncentrosymmetric model, x moved close to $\frac{1}{2}$ to eliminate the calculated differences between $I(\mathbf{h})$ and $I(\bar{\mathbf{h}})$. The parameters obtained for the refinements of the Friedel pairs measured with Mo $K\alpha$, using the $Pnma_{des}$ model ($R = 0.0366$, $wR = 0.0504$ and $S = 2.25$), are better than those found using the $Pn2_1a_{des}$ model ($R = 0.0428$, $wR = 0.0540$ and $S = 1.76$), even though the total number of parameters increases from 56 to 100. This set of results leads to the conclusion that the disordered *Pnma* space group is indeed the most accurate to describe the macroscopic symmetry of the crystal.

Raman spectroscopy experiments performed in the INC phase gave approximately the same results as those obtained in the RT phase. As a consequence, a similar strategy was used in the study of the RT phase and in the study of the average structure of the incommensurate phase (INC_{av}). The parameters obtained in the refinements of the Ag $K\alpha$ data are listed in Table 3; refinements performed in $Pn2_1a_{ord}$ and $Pnma_{ord}$ models in the RT phase are shown for the sake of comparison. The atomic coordinates and U_{eq} parameters are listed in Table 4.† The atomic arrangement in the RT phase can be seen in Fig. 2 (Burnett & Johnson, 1996; *ORTEP*III), with the structure in the INC_{av} phase being very similar. The distance between similar Br atoms in two related tetrahedra lies in the range 0.2–0.5 Å.

3.2. *Modulated phase characterization*

The existence of a modulation between 245 and 233 K was evidenced by the presence of many weak satellite reflections at $\mathbf{H} = (h + q)\mathbf{a}^* + k\mathbf{b}^* + l\mathbf{c}^*$. Owing to the low intensity of the satellites only very few of them could be centered by the usual processes, giving $q \simeq 0.16$. In order to optimize the value of q an alternative process was employed. For each temperature the lattice parameters were determined as described in §2. After this, slow ω scans around $\mathbf{H} = (h + 0.16 + \delta_i)\mathbf{a}^* + k\mathbf{b}^* + l\mathbf{c}^*$, with different values of δ_i, were performed and the center θ_i of each profile was determined by a least-squares fit using Voigt curves. The average value of θ was used to calculate the value of q with $|\mathbf{H}|^2 =$

† Lists of anisotropic displacement parameters and structure factors have been deposited with the IUCr (Reference: SH0100). Copies may be obtained through The Managing Editor, International Union of Crystallography, 5 Abbey Square, Chester CH1 2HU, England.

Table 4. *Fractional atomic coordinates (Å) and equivalent isotropic displacement parameters (Å^2) in the different phases of Cs_2HgBr_4*

The results concern the measurements performed using Ag $K\alpha$ ($\lambda_{Ag\ K\alpha}$ = 0.5609 Å); p represents occupation parameter and $U_{eq} = (1/3)\Sigma_i\Sigma_j U^{ij} a^i a^j \mathbf{a}_i \mathbf{a}_j$.

	p	x	y	z	U_{eq}
RT phase, $Pnma_{des}$ (295 K)					
Hg	1.0	0.2215 (1)	1/4	0.4235 (0)	0.0529 (2)
Cs1	1.0	0.1207 (1)	1/4	0.099 (1)	0.1015 (6)
Cs2	1.0	−0.0173 (1)	1/4	0.6723 (1)	0.0619 (4)
Br1	1/2	−0.0263 (2)	0.2245 (23)	0.4096 (1)	0.0883 (34)
Br2	1/2	0.3212 (2)	0.2387 (21)	0.5933 (1)	0.0979 (16)
Br3	1/2	0.3296 (13)	0.5217 (20)	0.3537 (12)	0.0813 (25)
Br4	1/2	0.3098 (15)	0.4967 (23)	0.3263 (13)	0.1121 (46)
INC_{av} phase, $Pnma_{des}$ (235 K)					
Hg	1/2	0.2210 (1)	1/4	0.4236 (1)	0.0421 (3)
Cs1	1/2	0.1194 (2)	1/4	0.0993 (2)	0.0853 (10)
Cs2	1/2	−0.0167 (1)	1/4	0.6720 (1)	0.0499 (6)
Br1	1/2	−0.0266 (3)	0.2246 (43)	0.4097 (3)	0.0672 (61)
Br2	1/2	0.3221 (3)	0.2439 (29)	0.5938 (2)	0.0906 (21)
Br3	1/2	0.3292 (17)	0.5272 (25)	0.3577 (12)	0.0736 (41)
Br4	1/2	0.3111 (19)	0.4943 (24)	0.3226 (12)	0.0871 (53)
LT_1 phase, $P2_1/n$ (213 K)					
Hg	1.0	0.2210 (1)	0.2473 (2)	0.4245 (1)	0.0394 (2)
Cs1	1.0	0.1186 (1)	0.2584 (4)	0.1020 (1)	0.0790 (7)
Cs2	1.0	−0.0159 (1)	0.2597 (3)	0.6718 (1)	0.0450 (4)
Br1	1.0	−0.0278 (2)	0.2550 (6)	0.4103 (2)	0.0737 (10)
Br2	1.0	0.3242 (2)	0.2858 (5)	0.5930 (2)	0.0609 (11)
Br3	1.0	0.3246 (4)	−0.0333 (4)	0.3616 (3)	0.0689 (11)
Br4	1.0	0.3143 (4)	0.4890 (4)	0.3183 (3)	0.0768 (13)

$[2\sin\theta/\lambda]^2 = (h + q)^2\mathbf{a}^{2*} + k^2\mathbf{b}^{2*} + l^2\mathbf{c}^{2*}$. This procedure was repeated for different reflections in order to obtain the representative average value of q for that temperature. In spite of the experimental difficulties of this method and the large uncertainty in the individual values, a dependence of q with temperature [$q = q(T)$] could be registered (Fig. 3).

3.3. *LT_1 structure and INC ↔ LT_1 phase transition*

The LT_1 phase is observed below T = 233.7 K for Cs_2HgBr_4. Although the lattice parameters would indicate an orthorhombic symmetry for this phase, the observed extinction rules did not reasonably satisfy any orthorhombic space group; however, they satisfy the monoclinic $P2_1/n$ space group. Structure refinements of this phase using different disordered models failed. The best refinements were obtained using an ordered model in which the structure was described by two monoclinic pseudomerohedrally twinned domains, with a twin volume ratio of ~$\frac{1}{2}$. The agreement parameters of the refinements are presented in Table 3. Atomic parameters for the LT_1 phase refined in the $P2_1/n$ space

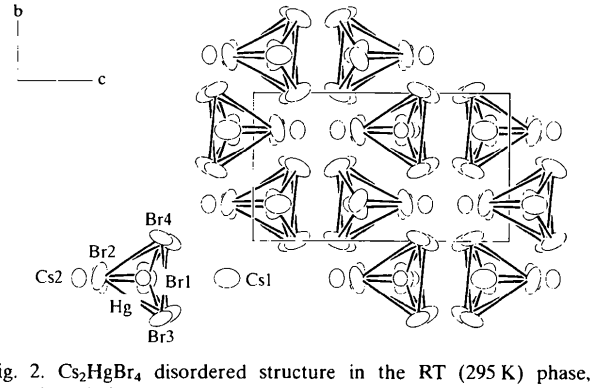

Fig. 2. Cs_2HgBr_4 disordered structure in the RT (295 K) phase, projected along the **a** axis.

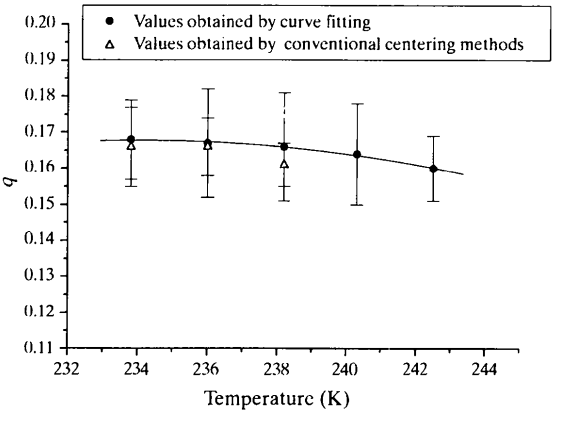

Fig. 3. Temperature dependence of the modulation vector. Values obtained by both the usual and alternative centering processes are indicated. The large uncertainty is due to the very low intensities of the satellite reflections.

group are listed in Table 4 and the atomic arrangement in the unit cell can be seen in Fig. 4.

The study of the behavior of some reflection intensities evidenced phase coexistence in the neighborhood of the INC $\leftrightarrow$ LT_1 phase-transition temperature, $229 < T < 232$ K. Fig. 5 shows the intensities of some main and satellite reflections near the 'lock-in' phase transition; it can be seen that while the main 120 and 160 reflection intensity increases, the satellite $3\bar{4}11$, 1601 and 1201 intensity decreases, but only becomes zero below 229 K. It should be noted that both 160 and 120 main reflections are forbidden in the INC phase according to its space-group symmetry.

4. Conclusions

The phase-transition sequence of Cs_2HgBr_4 has been confirmed by DSC experiments using both powder and single crystals, and the temperature values for each transition agree with the literature. Raman spectroscopy experiments evidenced the existence of disorder in Cs_2HgBr_4 crystals: an extra line corresponding to the ν_1 breathing mode of the $[HgBr_4]^{2-}$ tetrahedron was observed, but it should be absent if the structure was perfectly ordered. It might be emphasized here that disordered structures have been reported for several A_2BX_4 crystals, where each X atom can statistically occupy two distinct positions (Aleksandrov, 1993) and the degree of disorder is different for different compounds; in general, Fourier synthesis can not show a split in the X positions.

Generally, large atomic displacement parameters verified in refinements could be interpreted under considerations of disorder and/or thermal anharmonicity. In the present work no significant improvement was observed when anharmonic refinements, $B + \Gamma$ and $B + \Gamma + \Delta$, were compared with harmonic ones, only B, despite the increase in the total number of refined parameters (B, Γ and Δ represent the second, third and fourth rank displacement tensors, respectively). Moreover, the Fourier synthesis has shown atomic position splitting, even considering anharmonicity effects. By previous considerations it could be stated that only thermal effects did not justify some of the large atomic displacement parameters found in the refinements.

Statistical parameters obtained in different refinements of Cs_2HgBr_4 structures indicate the disordered model in the space group *Pnma* as more convenient to describe the RT and INC_{av} structures. The transition from the INC to the LT_1 phase occurs with a phase coexistence in a temperature interval of almost 4°. Raman experiments have shown that the disorder decreases with temperature, but only vanishes near $T = 100$ K, *i.e.* in the $LT_1 \rightarrow LT_2$ phase transition. The structure of the LT_1 phase is satisfactorily described in the space group $P2_1/n$ with two ordered twinned domains.

The main driving forces for the phase transitions in Cs_2YBr_4, Y = Hg and Cd, are the Cs $\leftrightarrow$ Br attraction and the Br $\leftrightarrow$ Br repulsion. In both compounds the phase transformations are described by a rotation wave through YBr_4 tetrahedra, which changes the environment of the Cs atoms (Altermatt *et al.*, 1984; Speziali & Chapuis, 1989). The cavities around the two Cs positions have different sizes, as can be seen by the large difference in the U_{eq} values of the Cs atoms. 11 Br atoms define the larger cavity around Cs1 and the smaller one around Cs2 is defined by nine of them. Considering that only Br atoms are affected by the disorder, the large difference in the U_{eq} parameters for Cs1 and Cs2 indicates that the $Cs^+ \leftrightarrow [HgBr_4]^{2-}$ interaction is different for each Cs atom. This difference would modify the electric potential, allowing the bromide tetrahedron to choose two or more orientations in the structure, which gives rise to the disorder verified in RT and INC phases. In the LT_1 phase the difference between the $Cs2^+$ and $Cs1^+$ interaction with the $[HgBr_4]^{2-}$ tetrahedron is very small and the split in the Br positions is not large enough to be solved by X-ray refinements.

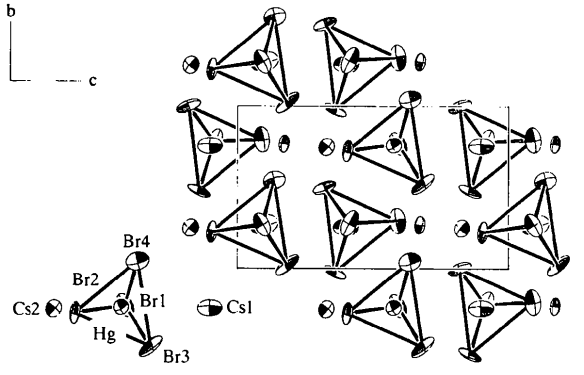

Fig. 4. Cs_2HgBr_4 structure in the LT_1 (213 K) phase, projected along the **a** axis.

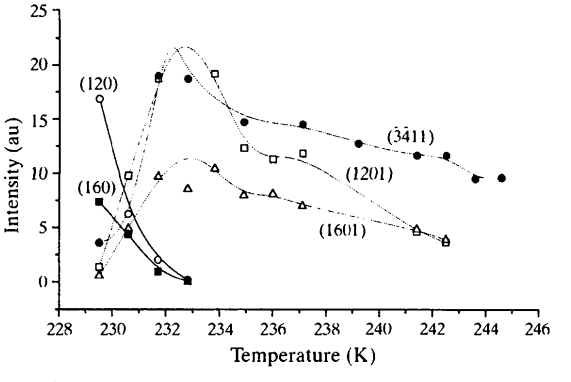

Fig. 5. The intensity behavior of satellite and main reflections as a function of temperature, near the INC $\leftrightarrow$ LT_1 phase transition, during the cooling process. The intensities were calculated by adjusting the profiles using Voigt curves.

The appearance of the main reflection in the INC phase characterizes a transition through the multi-soliton limit. In other words, throughout the phase coexistence region, parts of the crystal change from the INC phase to commensurate. Once the LT_1 commensurate phase is twinned, it can be stated that in the coexistence temperature range the $[HgBr_4]^{2-}$ tetrahedron chooses one of the two extreme modulated configurations with $q(T)$ suddenly jumping from $\mathbf{q}(T) = 0.168\mathbf{a}^*$ to $q(T) = 0$.

According to all the results presented here the phase-transition sequence for Cs_2HgBr_4 would be summarized as follows

Pnma		*Pnma*		$P2_1/n$		?		?
Disordered		Disordered						
$\longrightarrow$	T_1	$\longleftrightarrow$	T_2	$\longleftrightarrow$	T_3	$\longleftrightarrow$	T_4	$\longleftrightarrow$.
	(245 K)		(233 K)		(167 K)		(85 K)	
RT		INC		LT_1		LT_2		LT_3
		$\mathbf{q} \simeq 0.165\mathbf{a}^*$		Twinned				

In RT, INC and LT_1 phases only four molecules were necessary to describe the unit cell ($Z = 4$) and no unusual distances or angles were observed; small changes in the internal structure of $[HgBr_4]^{2-}$ tetrahedra are not significant.

The crystals used in this work were kindly provided by Professor H. Arend. The authors would like to thank to Dr Howard Flack and Dr Vaclav Petricek for the helpful discussions. This work was partially supported by FAPEMIG (Fundação de Apoio à Pesquisa do Estado de Minas Gerais, Brazil) and CNPq (Conselho Nacional de Desenvolvimento Científico e Tecnológico, Brazil).

References

Aleksandrov, K. S. (1993). *Krystallografya*, **38**, 128–139.
Altermatt, D., Arend, H., Gramlich, V., Niggli, A. & Petter, W. (1979). *Mater. Res. Bull.* **14**, 1391–1396.
Altermatt, D., Arend, H., Gramlich, V., Niggli, A. & Petter, W. (1984). *Acta Cryst.* B**40**, 347–350.
Burnett, M. N. & Johnson, C. K. (1996). *ORTEP*III. Report ORNL-6895. Oak Ridge National Laboratory, Tennessee, USA.
Dmitriev, V. P., Yuzyuk, Y. I., Durnev, Y. I., Rabkin, L. M., Larin, E. S. & Pakhomov, V. I. (1989). *Sov. Phys. Solid State*, **31**, 770–773.
Fait, J. (1991). *XSCANS User's Manual.* Siemens Analytical X-ray Instruments Inc., Madison, Winsconsin, USA.
Flack, H. D. (1983). *Acta Cryst.* A**39**, 876–881.
Jório, A. V., Dantas, M. S. S., Pinheiro, C. B., Pimenta, M. A. & Speziali, N. L. (1998). *Phys. Rev. B.* **57**, 203–209.
Pakhomov, V. I., Fedorova, N. M. & Ivanova-Korfini, I. N. (1978). *Koord. Khim.* **4**, 1765–1766.
Petricek, V. & Dusek, M. (1996). *JANA*96 *Crystallographic Computing System.* Institute of Physics, Academy of Sciences of the Czech Republic.
Semin, G. K., Alymov, I. M., Burbelo, V. M., Pakhomov, V. I. & Fedorov, P. M. (1978). *Izv. Akad. Nauk SSSR*, **42**, 2095–2100.
Speziali, N. L. & Chapuis, G. (1989). *Acta Cryst.* B**45**, 20–26.